ST-ECF Instrument Science Report WFC3-2005-07

Ground tests of the WFC3 NIR grisms

S. S. Larsen, H. Bushouse, J. R. Walsh
March 2005

ABSTRACT

The fundamental parameters of a slitless dispersing element are the geometrical configuration of the spectral orders, the dispersion relation relating pixel offset to wavelength and the sensitivity of each order. Based on thermal vacuum tests, the performance of the WFC3 near-IR G102 and G141 grisms has been assessed. The locations of the different orders relative to exposures taken through a direct imaging filter are determined, wavelength solutions are derived, and the relative throughput of the different orders is quantified. The wavelength solutions were found to be nearly linear functions of pixel offset for all orders and the tilt of the spectra to the pixel grid is 8 degrees for both grisms, but the grism test exposures were significantly out of focus.

1. Introduction

The Wide Field Camera 3 is fitted with three grisms for slitless spectroscopy. In the UVIS channel there is one grism G280L for the near-UV - visible range. The NIR channel has two grisms (G102 and G141) for the shorter and longer NIR wavelengths. The fundamental design parameters of a grism are the deflection of the incident beam by the grism (defined by the prism angle), dispersion in the various orders and the energy in each order (its sensitivity). In order to extract slitless spectra from grism images it is necessary to know these parameters and how they vary with position in the field. With a good parameterization, then extraction software, such as the aXe task developed at the ECF (http://www.stecf.org/~aXe), can be applied to extract multiple slitless spectra from sky images.

During the Thermal Vacuum (TV) testing of WFC3 in 2004, specific tests for the IR grisms were included. IR16S01 was the test procedure for G102 and IR16S02 the test for G141 (see Reid et al. 2004). Both sets of tests were designed to allow determination of the dispersion of the grisms through illumination by a monochromator of a pinhole (10 micron point target). The design band width of the monochromator was 10nm. It was planned to obtain the narrowband spectra at 20nm wavelength intervals for five apertures over the IR-channel field. In conjunction with these monochromator measurements, a dispersed white light spectrum would be taken at the same positions, in order to map the

spectrum tilt and trace. This ISR describes the implementation of this test and the analysis of the results. Tables provide the details of the spectral trace and the dispersion solution.

2. Test set-up

The IR16S01 and IR16S02 grism test procedures were executed on September 20-21, 2004, with the WFC3 in a flight-like thermal-vacuum environment. The WFC3 external optical stimulus system, CASTLE, was used to provide the necessary source targets for the tests. For these tests, the WFC3 IR detector was at an operating temperature of -123^{o}C and the IR Filter Select Mechanism (FSM) was at a temperature of -12^{o} C. The IR16S01 and IR16S02 test procedures use sets of point-source exposures, all of which were obtained with the CASTLE quartz-tungsten-halogen (QTH) lamp, and a 10 micron pin-hole to provide an unresolved target.

The out-of-focus images produced by both NIR grisms has been investigated by Bushouse & Hartig (2005). A series of focus sweeps of the external optical stimulus (CASTLE) showed that with CASTLE focus offsets of 5-10mm the same focus quality as the direct images (~1.4 pixels FWHM) could be achieved for the grisms, but the focus still remained to be a function of wavelength. The cause of the defocus has been traced to a 90 degree rotation error in the mounting of the NIR grisms in the filter wheel. In addition, there is a residual ~8 degree spectrum tilt (see section 4) that has also been traced to an error in the mounting procedures for the grisms (see Bushouse & Hartig 2005 and Turner-Valle 2005 for more details).

Table 1. *Log of G102 test exposures*

Filename	Grating/Filter	Target	Lambda center (nm)	Lambda width (nm)	Exptime (s)
ii160101r	F105W	center	cont.	-	20
ii160102r	G102	center	cont.	-	20
ii160104r	G102	center	800	10	10
ii160105r	G102	center	820	10	10
ii160106r	G102	center	840	10	10
ii160107r	G102	center	860	10	10
ii160108r	G102	center	880	10	10
ii16010ar	G102	center	900	10	10
ii16010br	G102	center	920	10	10
ii16010cr	G102	center	940	10	10
ii16010dr	G102	center	960	10	10
ii16010er	G102	center	980	10	10
ii16010gr	G102	center	1000	10	10
ii16010hr	G102	center	1020	10	10
ii16010ir	G102	center	1040	10	10
ii16010jr	G102	center	1060	10	10
ii16010kr	G102	center	1080	10	10
ii16010mr	G102	center	1100	10	10
ii16010nr	G102	center	1120	10	10
ii16010or	G102	center	1140	10	10
ii16010pr	G102	center	1160	10	10
ii16010rr	F105W	upper right	cont.	-	20
ii16010sr	G102	upper right	cont.	-	20
ii16010ur	G102	upper right	800	10	10
ii16010vr	G102	upper right	840	10	10
ii16010wr	G102	upper right	880	10	10
ii16010xr	G102	upper right	920	10	10
ii16010yr	G102	upper right	960	10	10
ii160110r	G102	upper right	1000	10	10
ii160111r	G102	upper right	1040	10	10
ii160112r	G102	upper right	1080	10	10
ii160113r	G102	upper right	1120	10	10
ii160114r	G102	upper right	1160	10	10
ii160116r	F098M	center	960	10	10
ii160117r	G102	center	960	10	10

Table 2. *Log of G141 test exposures*

Filename	Grating/Filter	Target	Lambda center (nm)	Lambda width (nm)	Exptime (s)
ii160201r	F139M	center	cont.	-	8
ii160202r	G141	center	cont.	-	20
ii160204r	G141	center	1100	10	10
ii160205r	G141	center	1150	10	10
ii160206r	G141	center	1200	10	10
ii160207r	G141	center	1250	10	10
ii160208r	G141	center	1300	10	10
ii16020ar	G141	center	1350	10	10
ii16020br	G141	center	1400	10	10
ii16020cr	G141	center	1450	10	10
ii16020dr	G141	center	1500	10	10
ii16020er	G141	center	1550	10	10
ii16020gr	G141	center	1600	10	10
ii16020hr	G141	center	1650	10	10
ii16020ir	G141	center	1700	10	10
ii16020jr	F139M	lower left	cont.	-	8
ii16020kr	G141	lower left	cont.	-	20
ii16020mr	G141	lower left	1100	10	10
ii16020nr	G141	lower left	1150	10	10
ii16020or	G141	lower left	1200	10	10
ii16020pr	G141	lower left	1250	10	10
ii16020qr	G141	lower left	1300	10	10
ii16020sr	G141	lower left	1350	10	10
ii16020tr	G141	lower left	1400	10	10
ii16020ur	G141	lower left	1450	10	10
ii16020vr	G141	lower left	1500	10	10
ii16020wr	G141	lower left	1550	10	10
ii16020yr	G141	lower left	1600	10	10
ii16020zr	G141	lower left	1650	10	10
ii160210r	G141	lower left	1700	10	10
ii160211r	F139M	lower left	1390	10	10
ii160213r	G141	lower left	1390	10	10

3. Measurements

Logs for the test exposures for G102 and G141 are given in Table 1 and Table 2 respectively. For each grism a series of spectra of a monochromator source were obtained, as well as spectra and direct images of a continuum source. Test exposures were obtained for two locations of the target beam, one approximately centered on the detector and one near a corner. This approach was intended to allow a first-order assessment of any field dependence of the trace- and wavelength relations. For the G102 grism, monochromator spectra were obtained for the range 800 nm - 1160 nm in steps of 20 nm (for the central beam) and in 40 nm steps for the corner beam. Unfortunately, for the corner beam (upper right) the rotation error of the grisms caused the 1st order G102 spectrum to fall outside the detector area. However, the -1st order could be seen. For G141 the corresponding wavelength range was 1100 nm - 1700 nm with 50 nm steps, and the lower left rather than the upper right corner was chosen so that the 1st and 2nd (and even the 3rd) orders were comfortably within the detector area. In all cases, the monochromator bandwidth was 10 nm.

Figure 1: *Sum of the direct image (F105W) and G102 exposure of the continuum source. The direct image is marked by a circle, and the grism +1st order can be seen extending towards the right. The grism 0th order is also visible as a point source to the left of the direct image.*

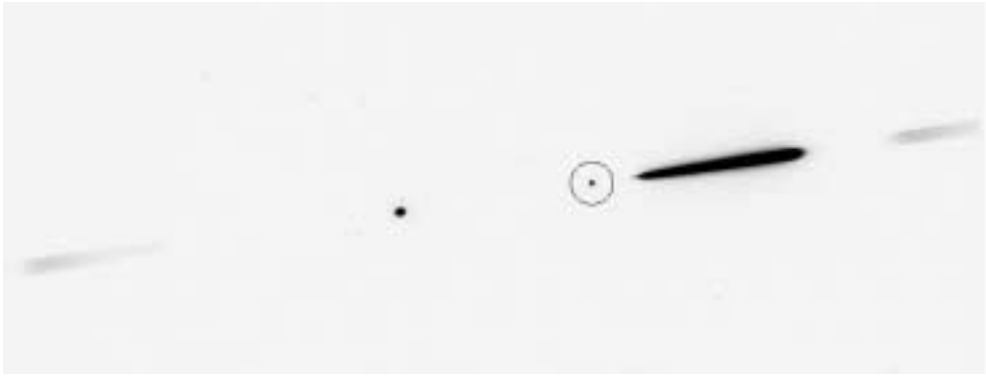

Figure 2: *Sum of the direct image (F139M) and G141 exposure of the continuum source. The direct image is marked by a circle, and the grism +1st and +2nd orders can be seen extending towards the right. To the left of the direct image are the grism 0th and -1st orders. It is evident that all orders are significantly out of focus.*

Figure 1 and Figure 2 show sums of the direct (F105W/F139M) images and the continuum grism spectra for the central beam location for grisms G102 and G141 respectively. No dark exposures were obtained, but for the purpose of these two figures we have subtracted a dark frame constructed by median-combining all the monochromator spectra and scaling them according to exposure time. In both figures the direct image is marked by a circle, and the 1st order can be seen extending towards the right (increasing detector X-values). The 0th order grism spectra can be seen as nearly point-like sources to the left of the direct images. In the G141 exposure the +2nd and -1st orders are also faintly visible, but these are both much fainter than the +1st order.

4. Analysis

The datasets containing spectra, listed in Tables 1 and 2, were analysed. Bias was subtracted from the images, the orders were traced and dispersion solutions fitted to the measured positions of the monochromator spots versus wavelength as listed in column 4 of Tables 1 and 2. As noted above, no dark exposures were obtained, although for the very short exposure times used in these tests the dark current is not significant.

Tracing the spectral orders

The ST-ECF aXe package for reduction of slitless spectroscopy data treats the spectral traces and wavelength solutions defined with respect to the position of the source in the direct image. The centroids of the continuum source images in the direct imaging expo-

sures (X_{ref}, Y_{ref}) were determined by running SExtractor. These positions were assumed not to change through the duration of the remaining measurements.
The first-order spectra were traced by measuring the centroid across the continuum spectra, using a custom-written C program. We found the traces to be well fit by straight lines, with very little if any offset between the best-fitting straight lines and the direct images. Because of the significant departures from optimal focus, it was difficult to carry out meaningful fits to other than the +1st orders, so for the other orders we simply defined the traces by drawing straight lines through the direct image and some reference point on the order. Our adopted trace descriptions are given in Table 3. For both the G102 and G141 grisms, the angle between the dispersion direction and the detector X-axis is about 8.5 degrees. In the case of G141 we find a slight field dependence, while for G102 the data does not allow us to quantify any field dependence.

Table 3. *Trace descriptions. The traces are assumed to be of the form ($Y-Y_{ref}$) = DYDX_0 + DYDX_1 * ($X-X_{ref}$), where (X_{ref}, Y_{ref}) are the coordinates of the source in the direct image. The ($X-X_{ref}$) ranges given here are only approximate*

Order	($X-X_{ref}$) range	DYDX_0	DYDX_1
G102, center			
+1	0..300	-0.209	0.1499
0	-300..-250	0.0	0.1429
G102, corner			
-1	-800..-600	0.0	0.1569
G141, center			
+1	0..270	-0.630	0.1495
+2	270..475	0.0	0.1457
0	-220..-170	0.0	0.1520
-1	-610..-420	0.0	0.1491
G141, corner			
+1	0..270	-0.577	0.1312
+2	270..475	0.0	0.1310
+3	475..659	0.0	0.1296
0	-220..-170	0.0	0.1332

.

Dispersion solutions

The trace definitions were inserted into a configuration file for the aXe spectral extraction software and each of the monochromator spectra were then extracted using the standard aXe tasks (SEX2GOL, GOL2AF, AF2PET, BACKEST, STAMPS and PET2SPC). These tasks automatically extract the spectral orders as separate “beams”, defined with respect to the location of the object in the direct image. A wide extraction box extending to +/-15 pixels on both sides of the trace was used, thus ensuring that most of the flux was included in spite of the poor focus. The FITS spectra produced by aXe were then converted to IRAF format (using the TDUMP and RSPECT tasks in IRAF) and the ($X-X_{ref}$) location of the peak of each monochromator spot was measured by carrying out a Gaussian fit to the extracted spectrum using the SPLOT task in the ONEDSPEC package in IRAF. In the case of the -1st order of the G102 spectra, the spectra were so much out of focus that Gaussian fits were not possible, and the approximate emission peaks were simply estimated by eye.

The wavelength solutions were found to be well approximated by linear fits to Lambda versus pixel offset, with the coefficients listed in Table 4. The errors given in the table are from linear least-squares fits (carried out with the POLYFIT task in IRAF). The table also lists the number of fitted data points for each order, which is often quite low for the higher-order terms. This is due to the poor focus combined with generally low throughput of higher orders, which made it difficult to measure more than a few datapoints. A statistically significant quadratic term was found only for the G141 1st order, but even here the maximum difference between the best linear and quadratic fits amounts to less than 1 nm over the 1100 nm - 1700 nm wavelength range.

Within the uncertainties, the wavelength solutions behave as expected, with the +1st and -1st orders having similar dispersions, and the +2nd and +3rd orders having dispersions of 1/2 and 1/3 of that of the 1st order. The 0th order spectra also show a slight dispersion. For the G141 grism a comparison of the two beam locations allows us to quantify the field dependence of the dispersion solutions. We find that the dispersion varies by about 4% between the field center and the lower left corner for the +1st and +2nd orders.

Table 4. *Dispersion solutions, assumed to be of the form Lambda(nm) = DLDP_0 + DLDP_1 * (X-X_{ref})*

Order	DLDP_0	DLDP_1	N (fit)
G102, center			
+1	637.82 +/- 0.55	2.158 +/- 0.003	19
0	31827 +/- 1736	111 +/- 6	17
G102, corner			
-1	-1290 +/- 797	-3.13 +/- 1.06	4
G141, center			
+1	877.18 +/- 0.47	4.084 +/- 0.003	13
+2	454.2 +/- 3.4	2.009 +/- 0.010	4
0	53955 +/- 1089	259.5 +/- 5.4	11
-1	-960.7 +/- 11.9	-4.529 +/- 0.022	12
G141, corner			
+1	873.63 +/- 0.32	4.253 +/- 0.002	13
+2	451.6 +/- 2.6	2.092 +/- 0.007	6
+3	340.53 +/- 0.06	1.3236 +/- 0.0001	3
0	53113 +/- 1132	265.0 +/- 5.8	12

Flux in different orders

In Figure 3 we show the counts in the +1st order for the G102 and G141 grisms. For G141 we show both the data for the central beam (solid line) and the corner beam (dotted line). As seen from the figure, the two grisms cover the wavelength range from 800 - 1800 nm without any gap, and both grisms show reasonably smooth count rates as a function of wavelength apart from a slight depression at about 1400 nm for G141. The spectrum of the quartz-tungsten lamp used for the illumination is very smooth, but the transmission curve of the fibers has a dip at 1400 nm, corresponding to the feature seen in the figure.

The relative flux in the different orders was estimated by adding up the counts in the monochromator spectra for the central beam location at each wavelength. Figure 4 and Figure 5 show the flux in the various orders as a function of wavelength, relative to all orders that were measured. For G102, only the 0th and 1st orders could be measured, while the -1st, 0th, +1st and +2nd orders were measured for the G141. For both grisms, the +1st order contains the majority of the flux at most wavelengths, with less than 10% in the remaining orders.

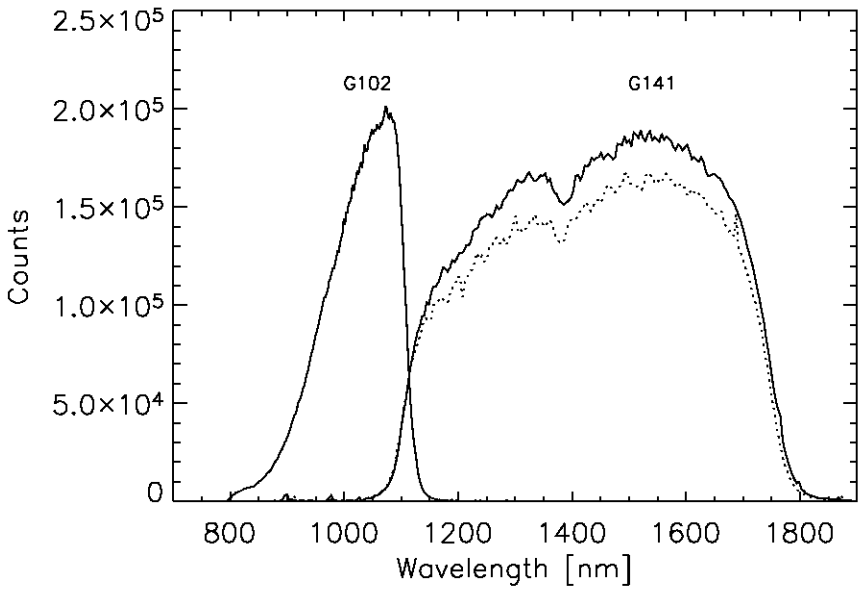

Figure 3: *Counts in the +1st order for G102 and G141 grisms. In the case of G141 both the central and corner data are shown.*

For G102, the relative flux in the +1st and 0th orders are 98.8% and 1.2% over the 800 nm - 1150 nm wavelength range. Using the upper right corner beam for a crude measurement of the flux in the -1st order, we estimate that this contains less than 1% of the flux over the 1000 nm - 1120 nm wavelength range. In the case of G141, the +1st, 0th, +2nd and -1st orders contain about 91.4%, 1.2%, 2.9% and 4.5% over the 1100 nm - 1700 nm range. Again, we use the corner beam measurements for a crude assessment of the +3rd order contribution, which is less than 1% over the range 1100 nm - 1200 nm.

Finally, the throughput of the grism exposures relative to a direct imaging exposure was estimated. For G102, a direct image through the F098M filter and grism spectra were obtained for a monochromator setting of 960 nm. Within an R=20 pixels aperture, the counts in the +1st order grism exposure spectrum were 83% of those in the direct image. For G141 a similar procedure was followed, using the F139M filter and a 1390 nm monochromator setting. Here, the counts in the +1st order grism spectrum were found to be about 86% of those in the direct image.

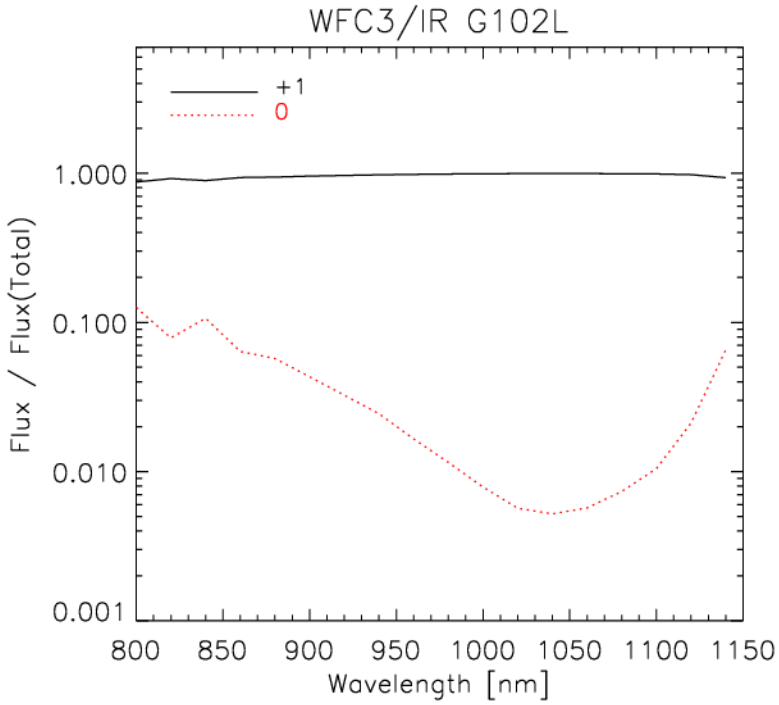

Figure 4: *Fractional flux in the 0th and +1st orders for the G102 grism.*

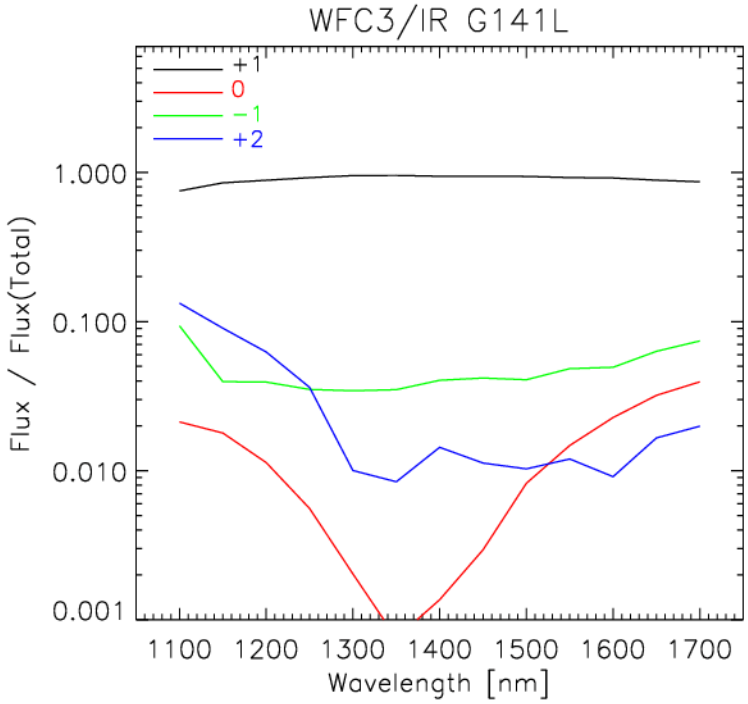

Figure 5: *Fractional flux in the +1st, +2nd, 0th and -1st orders of the G141 grism, relative to the total flux. The +1st order contains the majority of the flux at all wavelengths.*

Focus variations

The main difficulty encountered during the IR grism TV tests was the poor image quality, caused by a focus shift of the grisms relative to the direct images. Figure 6 and Figure 7 show cuts across the 1st order G102 and G141 spectra at three different positions along the trace, near the blue end, center, and red ends of the orders. Also shown are the profiles of the direct image exposures. The direct images in both cases have FWHM of about 1.4 pixels. For the G102 1st-order grism spectra the FWHM varies between 6.4 pixels (at 840 nm) to 10.0 pixels (at 1140 nm), and for G141 the range is between 2.6 pixels at 1100 nm and 7.3 pixels at 1700 nm. Full details are given in Bushouse & Hartig (2005). Correction of the grism mounting errors is expected to solve this problem.

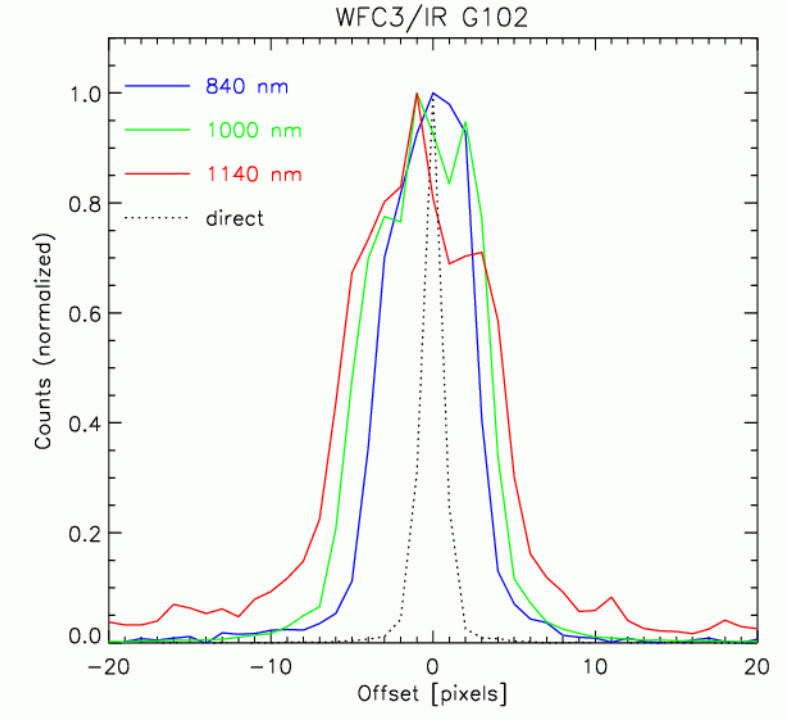

Figure 6: *Cut across columns for three positions along the 1st-order G102L spectrum.*

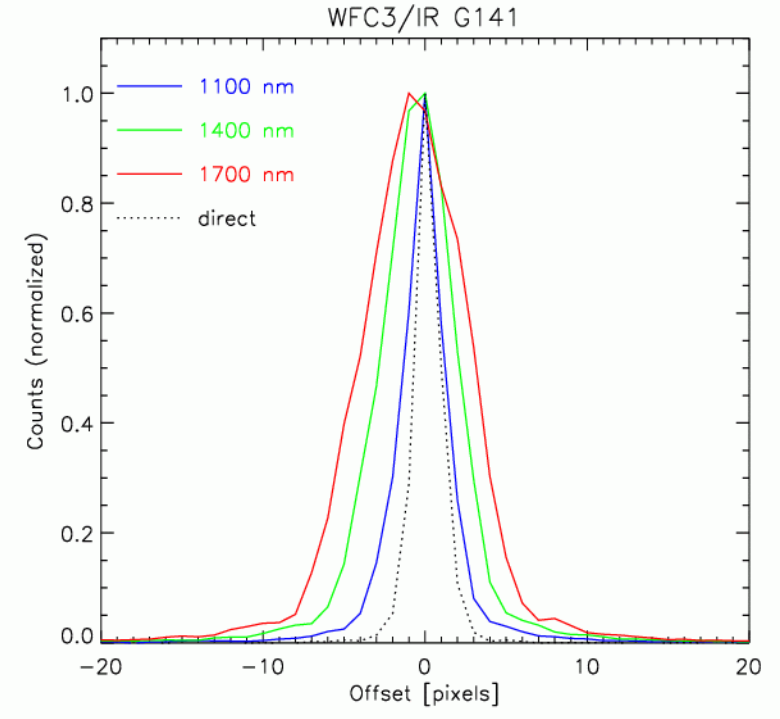

Figure 7: *Cut across columns for three positions along the 1st-order G141L spectrum*

5. Conclusions

Thermal vacuum tests have been carried out for the WFC3 IR-channel G102 and G141 grisms. Both grisms show nearly linear dispersion relations and trace definitions, with the first-order spectral traces passing through direct imaging exposures within an accuracy of better than one pixel. For both grisms, more than 90% of the total flux is in the +1st order spectra. The dispersion direction is tilted by about 8.5 degrees with respect to the detector X-axis, but this can be easily handled within the aXe package. This tilt has been traced to a residual rotation error in the mounting of the IR grisms in the filter wheel (see Turner-Valle 2005) and is expected to be reduced to less than 1 degree by remounting the grisms. We conclude that the grisms in the WFC3 IR channel are well suited for high-quality slit-less spectroscopy, provided that the focus problems are solved.

Acknowledgements

We thank W. Freudling for helpful comments

References

Reid, I. N., Bartko, F. Baggett, S., Brown, T., Bushouse, H., Hartig, G., Hilbert, B., Lupie, O., Robberto. M., Stiavelli, M., 2004. *WFC3 Science Calibration Plan. Part 4: Test Procedures*. ISR WFC3 2004-03

Bushouse, H., Hartig, G. F., 2005. *WFC3 Thermal Vacuum Testing: IR Grism Focus and Tilt Anomalies.* ISR WFC3 2005-06

Turner-Valle, J., 2005. *WFC3 IR Grism Modeling and Rotations*. Ball Aerospace Systems Engineering Report (SER) OPT-079.